JOURNAL OF SOLID STATE CHEMISTRY 88, 269–277 (1990)

Phase Transitions Induced in Layered Host Structures during Alkali Metal Intercalation Processes

ERIC SANDRÉ, RAYMOND BREC,[1] AND JEAN ROUXEL

Laboratoire de Chimie des Solides, Institut de Physique et Chimie des Matériaux, 2 rue de la Houssinière, 44072, Nantes Cédex 03, France

Received March 5, 1990

DEDICATED TO J. M. HONIG ON THE OCCASION OF HIS 65TH BIRTHDAY

Intercalation processes are mostly considered from the host structure point of view in layer phases of the dichalcogenide MX_2 type or closely related to it. Host structure changes are shown to be linked either to true structural transition or to progressive alteration of the host network. These modifications concern three main fields: (i) the sliding motion of slabs with respect to each other; (ii) the changing of sites of the host framework cations; and (iii) the modifications associated with anion shift. Many examples are given which belong to the alkali metal intercalates A_xMX_2 family (M = Ti, Zr, Mo, Fe; X = O, S, Se; A = Li, Na, K) and to the structurally related thiophosphate intercalates Li_xMPS_3 (M = Fe, Ni, Cd, Mn).

I. Introduction

Intercalation of guest cations in a given host structure is usually written under the form of a classical topochemical reation:

$$xA^{n+} + xne^- + \text{Host} \rightarrow A_x\text{Host}^{(nx-)},$$

which expresses well that it is a coupled and reversible ion–electron transfer reaction. This equation gives the impression that the host structure plays a rather passive role, supplying only host sites and redox centers. Also, the true reversibility of the reaction may be questioned through the difference of scale between the microscopic molecular and the solid state macroscopic scale of the reaction in which interactions and correlations are so important. These latter factors may trigger intercalation-induced structural changes in the host (often underconsidered in the corresponding works). In this paper, a critical discussion of such structural changes on the basis of recent results on various systems is given, and with the help of some theoretical approach of the intercalation reaction. In fact, both the ion and the electron transfers may induce phase transitions or structural modifications in the host framework, separately or through more complex ion–electron-coupled effects. One can distinguish among phase transitions dealing with

—a sliding motion of slabs with respect to each other;

—a changing of sites of the host framework cations;

[1] To whom correspondence should be addressed.

0022-4596/90 $3.00

—modifications associated with anions of the host.

II. Sliding of Slabs

Slab gliding is linked to a coordination change around the guest species. The host network is not modified for the most part, that is to say, as far as its slab structure is concerned. Such gliding motions have been essentially related to the achievement of the most stable surrounding of the guest environment. A more subtle distinction should certainly be made depending on whether we are, or are not, dealing with a conductive compound. Delocalized wave functions that allow a better screening of extra charges will help to maintain the slab integrity. It is worth noting that all the slab alteration that has been observed up to now, and is discussed below, is related to localizing host structures.

Before describing the evolution when going from lithium to cesium, one must also remember the developed quantic behavior of lithium atoms which obey the law of minimum energy for the equilibrium state, and the rather classical behavior of bigger atoms which will follow the law of least action which may leave particles in a metastable state (Einstein model). In fact, big particles may remain in a metastable equilibrium state (classical mechanics principles) when small particles go directly to the lower energy state (quantum mechanics principles).

For instance, in a typical layered material such as TiS_2, the empty octahedral sites between the slabs are progressively filled in Li_xTiS_2 according to a progressive CdI_2–NiAs evolution. Sodium in Na_xTiS_2 also occupies octahedral sites but only for the higher values of x (0.78–1). For lower sodium content, the Na^+ ions occupy trigonal prismatic sites resulting from a shifting of one TiS_2 slab with respect to its neighbors. For larger alkali metal cations (K, Rb, and Cs), trigonal prismatic sites are found (*1*). Such a structural evolution, observed in all the systems, can be explained, in a first approach, through the role of three factors: the size of the alkali metal, the amount of intercalation, and the nature of the slabs of the host (*2*). In effect, an octahedron can accomodate higher charges on the anions than a trigonal prism does, hence the best balance between six similar charges. Thus, for a given alkali metal, assuming a complete ionization of the guest metal, the octahedral form will appear for higher intercalation rate. This is indeed the case of Na–TiS_2. It appears clearly also that with a big alkali metal, which makes the sulfur layers more distant from each other, the trigonal prismatic arrangement becomes more and more stable. The last factor involves the covalency of the host: ZrS_2, more ionic than TiS_2, will rather favor the octahedral structure, and, for instance, $KZrS_2$ is octahedral whereas $KTiS_2$ is trigonal prismatic.

It can be pointed out that such transitions, if repeated, may lead to an amorphization of the host structure. When intercalating electrochemically, for example, after a few cycles, a two-phase region emf plateau may disappear. This is due to a disorganization of the stacking in the host structure. The slabs must shift during the intercalation process and behave more and more independently from each other. Finally, one gets to some one-dimensional amorphous situation (along the direction perpendicular to the slabs) with no visible plateau in an electrochemical discharge curve. This is the case of the so-called pseudo-monophased systems. It allows the use of some initially biphased systems in batteries. A drawback is the difficulty in ascertaining phase limits through electrochemistry except when considering the first discharge curve. An example is provided by the Na–TiS_2 system.

A phase transition modifies the host structure and costs extra elastic energy in addition to the pulling apart of the slabs. The energy change expression to be associated

with the intercalation process is complex because it implies many terms such as the Madelung energy variation, the anionic polarization if the alkali metal is small, and the configuration entropy. These factors have to be taken into account along with the two essential effects of the elastic costs and of the electronic energy gain stemming from the initial and final energy levels for the electronic transfer reaction. When the gain in electronic energy overcomes the cost in distortion energy (there lies the driving force for intercalation chemistry), intercalation can take place. If the intercalation simply results in a continuous filling of octahedral sites between host slabs (CdI_2 to NiAs evolution), it may start from the very beginning ($x = 0$). This is well-illustrated by the Li–TiS_2 and Li–$ZrSe_2$ systems. In the case of a shifting of slabs, the intercalation does not start at $x = 0$, but at a minimum value x_{min}. This value probably translates the fact that it is necessary to transfer a sufficient number of electrons to compensate for the elastic energy extra cost. For instance, in the Li–ZrS_2 system, the $3R$ octahedral structure ($NaHF_2$), which implies a shifting of the slabs, is observed for $x > 0.25$. The only difference with $LiTiS_2$ is this slab gliding which gives the *ABC* sulfur slab succession (CFC type) instead of the *AB* one (HC type). It should be possible to go farther in these kinds of considerations. In effect, the shifts of the sheets with respect to each other must be respective to the more or less accentuated ionic character of the structure. This can be seen through the anisotropy of some physical properties in a direction perpendicular or parallel to the slabs. The separation of the sheets is actually directly related to the more or less ionic character of the compounds. It should be hence possible to relate x_{min} to the M–S bond ionicity. Things are in fact less simple because one should have perfectly comparable series of phases to eliminate other factors able to play a role. In any case, this idea that an x_{min} value is imposed to answer to a situation involving a host lattice modification is backed up by the study of systems in which a Jahn–Teller distortion would be totally or partially raised or created by the electronic structure changes induced by the electronic transfer. Indeed, if Jahn–Teller distortions are involved, inducing strains in the host lattice, largely biphased systems A_xMS_2 (x very small or zero)–A_1MS_2 will be observed. One could also suppose that the slabs do not allow the simultaneous occurrence of distorted and undistorted sites.

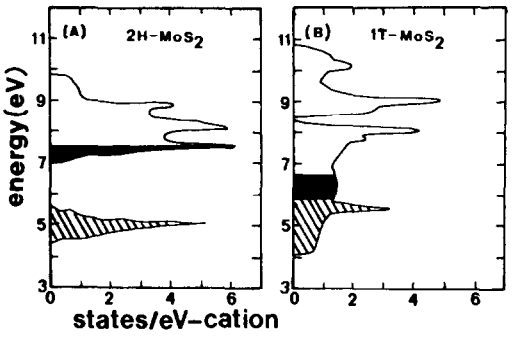

FIG. 1. Comparison of d-band density of states for 2H–MoS_2 and hypothetical 1T–MoS_2. The hatched region corresponds to occupied states; the blackened region shows the additional states filled in 2H–$LiMoS_2$ and 1T–$LiMoS_2$ (*3*).

III. Symmetry Change around the Host Network Cation

The slabs of the layered structure of 2H–MoS_2 are built up from a condensation of trigonal prisms MoS_6. The D_{3h} symmetry around molybdenum yields a splitting of the d levels with a stabilized a_1' level essentially built up from the d_{z^2} orbitals of the metal, below an e' group (d_{xy}, $d_{x^2-y^2}$) and finally an e'' group (d_{xz}, d_{yz}). This is directly reflected in the band structure shown in Fig. 1. With two d electrons on molybdenum, one gets a filled d_{z^2} band. When intercalating, one would have to add one electron to a much

higher level which is rather destabilizing (blackened region on the figure). Indeed, what is observed is a change of symmetry around molybdenum leading to the so-called $1T$–MoS_2 with "octahedral" slabs like TiS_2 (*3*). This is achieved by translations of atomic layers. Now, the band structure is drastically changed. It presents a broad conduction band (largely based on d_{xy}, d_{xz}, d_{yz} cationic levels). The hatched region corresponds to states already occupied before intercalation. The blackened region shows the additional states filled when intercalating. There is clearly an important stabilization associated to the 2H → $1T$ transition upon insertion.

Before intercalation, the electronic structure associated to the 2H–MoS_2 is more favorable than the $1T$ one (compared hatched regions). However, the difference is rather small. Indeed, the fact that MoS_2 is not far from the frontier between trigonal prismatic and octahedral dichalcogenides is also manifested in the $a_H/2R_{X^{2-}}$ versus d_{T-X}/a_H diagram (see Fig. 2 for an explanation of the symbols) which is classically used to separate octahedral and trigonal prismatic regions. MoS_2 is close to the frontier between the two domains. A trigonal prismatic to octahedral coordination change of the structures is accompanied by an increase in the M–X bond ionicity. From that point of view also, it is not unexpected that lithium intercalation introducing that type of change would lead to a different coordination (*4*).

The structural transition is a sheer one, involving glide processes between molybdenum and sulfur planes of the same type as the one described for the 2H to $1T$ transition in TaS_2. Finally, it is worth noting that intercalating in MoS_2 leads to a d^3 electronic configuration on the transition metal in the MS_2 layers. There is no transition metal-layered dichalcogenide for that configuration which would have been that of manganese in an hypothetical layered MnS_2. The usual band

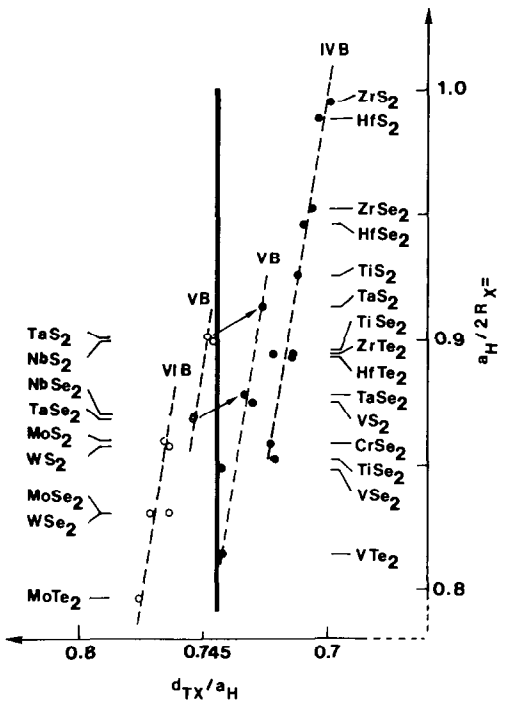

FIG. 2. Diagram of $a_H/2R_{X^{2-}}$ vs d_{T-X}/a_H, where a_H is the intralayer nearest-neighbor distance between chalcogen atoms, d_{T-X} is the chalcogen-transition metal bond distance, and R_X^{2-} is the chalcogen ionic radius. Note that $a_H/2R_{X^{2-}}$ is the measure of the charge on the chalcogen atom, whereas d_{T-X}/a_H is the evaluation of the distortion of the TX_6 polyhedra. From the example given, the transition from trigonal prismatic to octahedral coordination (from left to right) of T corresponds to decreased TX_6 distortion and increased ionicity (arrow) (see Ref. (*5*)).

structure scheme for MS_2 chalcogenides gives a clear explanation of that fact. When going to the right, the d levels are progressively lower. At a given moment, they may enter the sp valence band. If an empty d level is in that situation, it will be filled up at the expense of the sp valence band at the top of which holes appear. Chemically speaking, it means that the cation is reduced and the anions are oxidized under the formation of anionic pairs. This is the way one goes from layered TiS_2 with Ti^{4+} and $2S^{2-}$ to pyrites and marcassites with M^{2+} and $(S_2)^{2-}$

pairs. The d^3 electronic configuration for which octahedral symmetry was expected (no crystal field stabilization through a trigonal prismatic distortion) is finally achieved through a reduction of Mo^{4+} to Mo^{3+}, and not when trying to make an MnS_2-layered chalcogenide (MnS_2 has the pyrite structure).

IV. Changing of Host Cation Site

IV.1. The Cations Stay in the Slab of the Host

This case can well be illustrated by lithium intercalation in layered MPS_3 phases (*6*) with, for instance, M = Ni, Fe. The situation here is different from that of layered MX_2, because one starts in the pristine material with a very low oxidation state of 2+ for the transition metal, and the MS_2 slab becomes $SM_{2/3}(P_2)_{1/3}S$. One expects a substantially lowered stability for the cation for this type of phase, and indeed a high liability occurs with cations such as Cd^{2+} and Mn^{2+} (d^{10} and d^5 configuration) for which there is no crystal field stabilization in octahedral sites. They can be easily substituted at room temperature by a more ionic species (such as alkali metal) (*7, 8*). In the case of $NiPS_3$ one expects a reduction of Ni^{2+} by lithium, in agreement with the band structure of the phase (*9*). It was found that the higher occupied state is anionic and the lower unoccupied state is a cationic one; i.e., in those 2D chalcogenides, the last occupied state is essentially linked to pairs mostly localized in p_z orbitals of the chalcogen, whereas the first unoccupied state is a transition metal d state. Intercalation thus actually takes place according to the band structure scheme, and it has been demonstrated (*10*) that intercalation of lithium in $NiPS_3$ results in the complete reduction of the Ni^{2+} cations to Ni^0 according to

$$xLi + Ni^{2+}PS_3 \rightarrow Li_xNi^0_{x/2}Ni^{2+}_{1-x/2}PS_3.$$

The process seems to be a biphased one

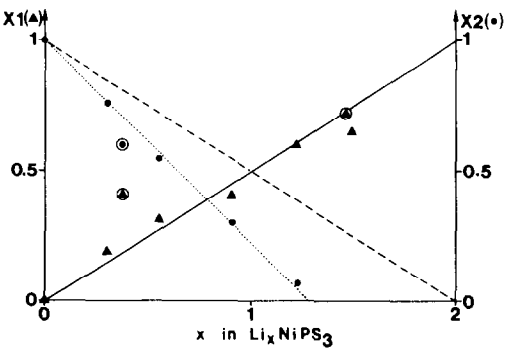

FIG. 3. Fitted fractions of nickel atoms in tetrahedral and octahedral sulfur environments (respectively $X1$ and $X2$). The straight line and the broken one correspond respectively to the fraction of reduced and unreduced nickel atoms.

with the occurrence, within the material, of reduced and unreduced regions corresponding to $NiPS_3$ itself and $Li_2Ni^0PS_3$. In the absence of any parameter change, one cannot say for the moment whether the system is truly (macroscopic) a two-phase one or if the separation of the domains takes place at a microscopic level, classifying the intercalates in that latter case as pseudo-phased according to A. Le Méhauté classification (*11*).

The intercalates are, at least at room temperature, kinetically stable, and their EXAFS spectra could be satisfactorily interpreted (*12*). They show that

—The reduction of Ni^{2+} into Ni^0 is a continuous phenomenon in the $0 < x < 1.5$ domain.

—The reduced nickel atoms are found in tetrahedral sulfur coordination, and their occurrence follows an $x/2$ law (see Fig. 3).

—The number of nickel atoms left in octahedral sites decreases accordingly.

—Two adjacent tetrahedral sites are filled at the same time by the migrant nickel and are located exclusively within the host slabs. This may allow the metal atoms to form nickel pairs (d_{Ni-Ni} = 2.45 Å).

—It is possible to suggest, for the totally

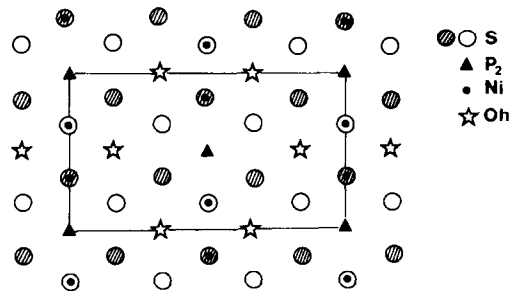

FIG. 4. Possible structure of the ($NiPS_3$) host slab of Li_2NiPS_3 for octahedral sites of the slab left by migrant nickel atoms.

reduced Li_2NiPS_3 intercalate, a structure which would correspond to the second phase of the Li_xNiPS_3 system (although this extreme intercalation composition cannot be reached without decomposition) (Fig. 4). This new structure is in agreement with the conservation of the cell parameters and its monoclinic space group ($C2/m$). It corresponds well to the unchanged spectra of the intercalates as compared to that of pristine $NiPS_3$. The very covalent nature of this type of phase (*13*, *14*) seems to exclude any metal shift due to charge redistribution, especially since the phenomenon starts from the beginning of intercalation (see below for host cation migration taking place for given lithium content in another type of ternary sulfides). One must then, as in the case of lithium intercalation in MoS_2, consider that the reduced transition metal achieved a better stability in a coordination different from that it has in the pristine phase, in agreement with the fact that the NiS_4 group corresponds to a drastic lowering of the ligand charge around the nickel atom. In Li_xNiPS_3, however, rather than a cooperative anionic and cationic glide motion, one observes a continuous cationic migration.

This result for $NiPS_3$ is in accord with the observation that Ni^0 is only known in a tetrahedral environment in organometallic compounds. If a two-electron reduction mechanism really takes place during lithium intercalation in $NiPS_3$, it is possible to put forward an explanation from an example given by the Mössbauer study of the $Li_x FePS_3$ intercalates. In that case, reduction of the $FePS_3$ matrix results also in the reduction of Fe^{2+} into Fe^0 which configuration corresponds to $3d^74s^1$ (*15*). It must be recalled that, in the pristine $FePS_3$ phase, the iron configuration was found to be $3d^{5.8}4s^{0.2}$ rather than the expected classical $3d^64s^0$ one. This has been interpreted as a partial transfer from electron pairs localized on $3p_z$ orbitals of sulfur of a slab toward iron cations in the adjacent slab through the van der Waals gap. Let us consider now a possible insertion mechanism, with the help of the schematic band dispersion of MPS_3 phases (Fig. 5).

(1) After an outer electronic solicitation at the surface, an electron pair of the gap (i.e., on S^{2-} $3p_z$) probably localized next to an impurity, jumps from the highest occupied state to a metal site in the opposite slab. A correlated hole would thus be created in the gap.

(2) Two lithium-donated electrons enter the host structure to combine with the holes.

(3) Li^+ ions can now diffuse in the structure to minimize the local excess charge due to the intercalation of the electron, thus compensating the defect. This step must be

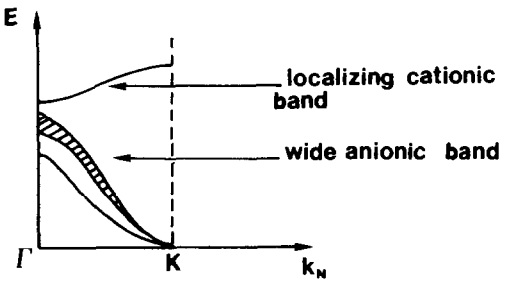

FIG. 5. Schematic band dispersion of the MPS_3 phases. The cationic lower band is flat due to its localizing character.

accompanied by local rearrangement as the diffusion is a slow step.

Beyond the relative stability of Ni^0 as compared to Ni^+, this may help explain the bielectronic mechanism observed in the reduction process of $NiPS_3$ and $FePS_3$.

This is the first example of a metal kinetically stable in its elemental state in sulfur coordination in an inorganic solid. It is also the second example, in the layered chalcogenide family, of a host structure modification upon reduction in relation with the change of ligand field stabilization.

IV.2. The Cations Move to the van der Waals Gap

IV.2.1. Case of the ternary oxides A_xMO_2. In the above phases, the layered structures are maintained, but there are some situations characterized by a movement of cations from a slab toward the adjacent van der Waals gap. This case is encountered when A_xMO_2, with layer MO_2 sheets, are disintercalated. In effect, one observes that the A_xMO_2 materials present atomic arrangements similar to the A_xMS_2 intercalation compounds, with, in particular, very stable transition metals in their octahedral environment. The alkali metal A^+ ions are intercalated between the O–*M*–O slabs and stabilize the whole structure. When removing the mobile A^+ ion while oxidizing the intraslab transition metal cation, this one is expected to maintain its local stability in its new higher oxidation state (at least from a coulombic point of view). Indeed, one observes a large disintercalation range, for instance, $x = 0.5, 0.5$, and 0.7 for the lower limit in the cobalt, nickel, and vanadium Li_xMO_2 derivatives (*16–19*). Beyond this value, the disintercarlation process reaches an irreversible domain, as one observes a moving of the M^{4+} cations toward the van der Waals gap where they replace partially the A^+ cations and stabilize the structure (Fig. 6). Such 2D → 3D structural changes are common to most of the A_xMO_2 systems. The Li_xCoO_2 system seems to have a different behavior, in relation with a cooperative intraslab ferroelectric displacement, that could ensure the stability through dipole–dipole interactions. In these examples, the host structure alterations differ from those observed in Li_xMoS_2, because the *M* cations maintain their coordination, in agree-

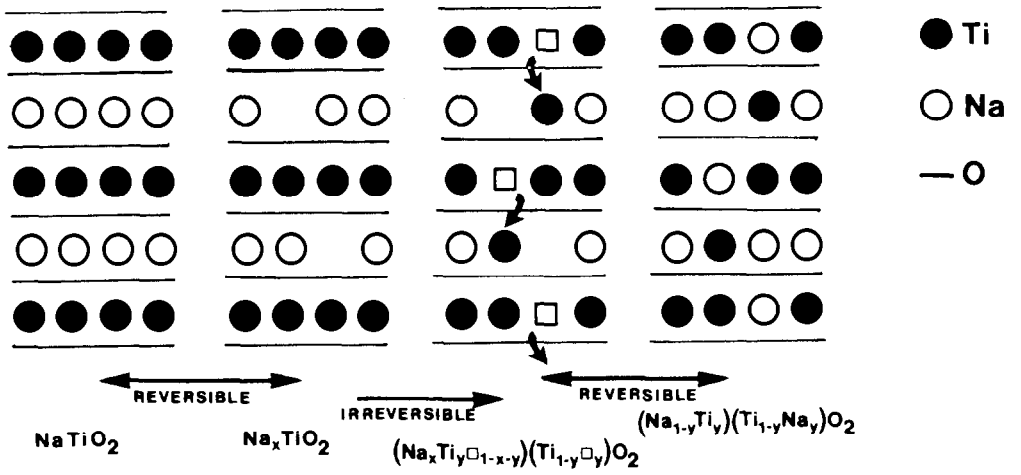

FIG. 6. Cationic rearrangement occurring in the reversible and irreversible disintercalations of $NaTiO_2$ (*7*).

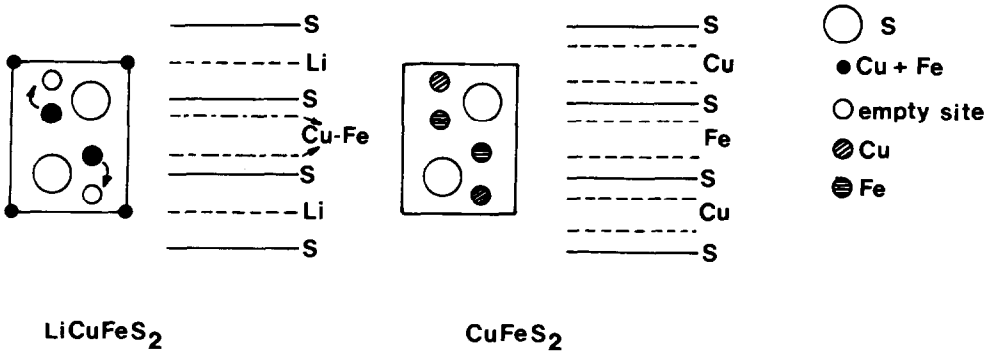

FIG. 7. Schematic representation in the (11–20) plane of the structure of the $LiCuFeS_2$ and Li_xCuFeS_2 ($0 < x < 1$). Arrows indicate the copper migration taking place when emptying the lithium site (at origin), from a Td site of the slab to the next one in the gap.

ment with the high stability of the M^{4+} and M^{3+} ions in octahedral surroundings. The above phases are highly ionic and the transition can surely be ascribed to increased electrostatic repulsions between adjacent oxygen layers with increasing disintercalation, the cation shift alleviating such repulsion. The cation displacement takes place at threshold values which should be related to the electropositivity of the M element. However, the question remains as to whether the system reacts for thermodynamic reasons or for kinetic ones and whether the new phases obtained are the most stable or only metastable.

IV.2.2. Case of $LiCuFeS_2$. The compound $LiCuFeS_2$, a recent phase prepared by R. Fong and J. R. Dahn (*20*), was found to have a hexagonal structure based on hexagonal closed packing of sulfur. Within one out of two sulfur layers, the tetrahedral sites are occupied half by Cu^+ and half by Fe^{2+}, whereas lithium fills the octahedral sites of the gap between the $CuFeS_2$ sheets. Disintercalation of lithium leads to nonstoichiometric Li_xCuFeS_2 phases, and a migration of copper, from an intralayer position to the interlayer one, was found to be concomitant with removal of lithium. The shifting cations maintain their coordination (see Fig. 7), and it can be assumed, like in the case of the double oxides above, that the copper displacement toward the structure's gap is related to charge redistribution in relation with coulombic energy stabilization. When all the lithium atoms are removed, a new hexagonal $CuFeS_2$ phase is obtained, adding a second form of the compound to the chalcopyrite.

V. Phase Transitions Involving the Host Anions

An example of this type of transition may be given by the Li_xFeS_2 system. It is possible to disintercalate the pristine Li_2FeS_2 phase in the $0 < x < 2$ range (*21*). Li_2FeS_2 has a structure made of a hexagonal close packing of S^{2-} anions with, in one slab, tetrahedral iron Fe^{2+} ions. Lithium ions are scattered for one-half on tetrahedral sites and for the other half on octahedral ones. Upon lithium removal, the oxidation of the host lattice takes place in two steps. The first one corresponds to the oxidation of Fe^{2+} into Fe^{3+}, the second one to that of some S^{2-} into S^-. Since S^- is not a stable species, one expects then the occurrence of sulfur pairing to constitute stable $(S_2)^{2-}$ entities. This phenomenon was well evidenced in the infrared spectra (550–200 cm^{-1}) of chemically oxidized Li_xFeS_2 samples, with the observation of the stretching vibration peak of the disulfide groups (*22*)

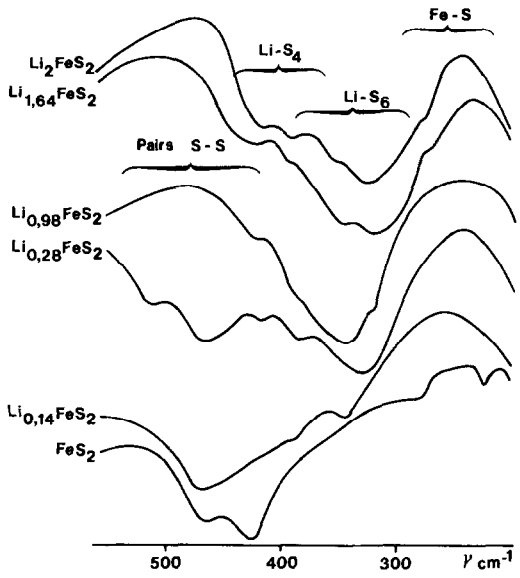

FIG. 8. Infrared absorption spectra of several Li_xFeS_2 phases showing, in the range 400–500 cm^{-1}, the occurrence of the S–S stretching vibration. From the Steudel relation (*23*), one can calculate two distances of 2.10 and 2.16 Å.

(see Fig. 8). Reintercalation of lithium allows has here an example of anionic positional shift during an oxidation–reduction process and, since the symmetry of the structure must change drastically (and contrary to the first step implying only an iron ion oxidation), one is dealing with a true phase transition accompanying the anionic movements.

VI. Conclusion

A few chosen examples have clearly shown that, in most cases, the rigid band model for studying intercalation effects is not quite appropriate. In many cases, the host structure undergoes very important changes with a not-so-quite irreversible character to be related either to entropic or to kinetic factors. Considering the few phase transitions and the continuous phase changing recorded in the given examples, we indeed must look at intercalation as a chemical reaction and not only as a physical process involving a diffusion followed by a gift of an electron to a static redox network.

References

1. A. LE BLANC, M. DANOT, L. TRICHET, AND J. ROUXEL, *Mater. Res. Bull.* **9,** 191 (1974).
2. J. ROUXEL, *J. Solid State Chem.* **17,** 223 (1976).
3. M. A. PY AND R. R. HEARING, *Canad. J. Phys.* **61,** 76 (1983).
4. R. BREC, *Mater. Sci. Eng. B* **3,** 73 (1989).
5. M. S. WHITTINGHAM AND A. J. JACOBSON (Eds.), "Intercalation Chemistry," Academic Press, New York (1982).
6. R. BREC, *Solid State Ionics* **22,** 3 (1986).
7. R. CLÉMENT AND M. L. H. GREEN, *J. Chem. Soc., Dalton Trans.* **10,** 1566 (1979).
8. R. CLÉMENT, *J. Chem. Soc. Chem. Comm. D,* 647 (1980).
9. M. H. WHANGBO, R. BREC, G. OUVRARD, AND J. ROUXEL, *Inorg. Chem.* **24,** 2459 (1985).
10. E. PROUZET, Thesis, Nantes (1987).
11. A. LE MÉHAUTÉ, R. BREC, A. DUGAST, AND J. ROUXEL, *Solid State Ionics* **3–4,** 185 (1981).
12. G. OUVRARD, E. PROUZET, R. BREC, S. BÉNAZET, AND H. DEXPERT, *SFC 88 J. Chim. Phys.* **86**(718), 1675 (1989).
13. M. EVAIN, Thesis, Nantes, p. 73 (1986).
14. M. BARJ, G. LICAZEAU, G. OUVRARD, AND R. BREC, *Eur. J. Solid State Inorg. Chem.* **25,** 449 (1988).
15. G. A. FATSEAS, M. EVAIN, G. OUVRARD, R. BREC, AND M. H. WHANGBO, *Phys. Rev. B* **35**(7), 3082 (1987).
16. L. A. DE PICCIOTTO AND M. M. THACKERAY, *Mater. Res. Bull.* **19,** 1497 (1984).
17. K. MIZUSHIMA, P. C. JONES, P. J. WISEMAN, AND J. B. GOODENOUGH, *Mater. Res. Bull.* **15,** 783 (1980).
18. M. G. THOMAS, W. I. DAVID, J. B. GOODENOUGH, AND P. GROOVES, *Mater. Res. Bull.* **20,** 1137 (1987).
19. C. DELMAS, *in* "Chemical Physics of Intercalation" (A. P. Legrand and J. Flandrois, Eds.), NATO-ASI Series B172, New York, Plenum, 209, (1988).
20. R. FONG AND J. R. DAHN, *Phys. Rev. B* **39**(7), 4424 (1989).
21. L. BLONDEAU, G. OUVRARD, Y. CALAGE, R. BREC, AND J. ROUXEL, *J. Phys. C: Solid State Phys.* **20,** 4271 (1987).
22. P. GARD, C. SOURISSEAU, G. OUVRARD, AND R. BREC, *Solid State Ionics* **20,** 231 (1986).
23. K. STEUDEL, *Angew. Chem. Int. Ed.* **14,** 655 (1975).